A Kinetics Formulation for Low-Temperature Plasticity

X.J. Wu and A.S. Krausz

The mechanism of low-temperature plastic deformation is controlled by thermally activated dislocation movements. An evolutionary constitutive law based on the principles of deformation kinetics is described in this article. The constitutive law is expressed with a sinh function designed for computational efficiency. It is derived from rigorously defined kinetics principles. The approximation involved in the sinh function is defined so that in applications an exact evaluation can be made of the validity limits. The system of the constitutive law and the external constraints lead to the operational equations. Applications are developed for constant strain-rate loading, constant stress-rate loading, stress relaxation, creep, and ratchetting processes. The analysis provides a unified treatment for low-temperature plastic deformation.

Keywords:
creep, dislocations, mathematical analysis, mechanical properties, plasticity: low temperature, testing

1. Introduction

THE mechanism of low-temperature plastic deformation (in the range of $T < 0.3\ T_m$, where T_m is the melting point) is controlled predominantly by the conservative motion of dislocations.[1-10] Krausz and Eyring[11] derived a rigorously expressed rate theory as the combination of forward and reverse activation steps over rate-controlling energy barriers and the associated kinetics description of thermally activated plastic deformation processes. The physically based deformation kinetics theory, as one of the two coupled equations of the constitutive laws of time- and temperature-dependent plastic deformation, is well established.[10] The constitutive law defines the behavior of the material: It is the description of the internal constraints. On this, the external constraint, the service condition of structures and machine elements or test method has to be imposed. This combination results in the operational equation that provides the mathematical description of the behavior in testing or for the design of components.

In testing and often in service of components, the typical external constraints are

- Constant strain rate
- Constant stress rate
- Stress relaxation
- Creep
- Ratchetting

The constitutive laws derived from deformation kinetics provide the physically rigorous expression of the behavior under these conditions, as well as under the effect of other external constraints, including the description of the effects of temperature and its variation during tests or in service.

X.J. Wu, Structures, Materials and Propulsion Laboratory, Institute for Aerospace Research, National Research Council of Canada, Ottawa, Ontario, K1A OR6 and **A.S. Krausz,** Department of Mechanical Engineering, university of Ottawa, Ottawa, Ontario, K1N 5NG.

2. The Rate Equation

In thermally activated dislocation motion, the rate of the process is defined by the rate of atomic bond breaking steps and by the changes in the interatomic distances and angles. The rate of each step is defined by the elementary rate constant:

$$\mathbf{k} = \nu \exp\left(-\frac{\Delta G^{\ddagger}(W)}{kT}\right) \qquad [1]$$

where ν is the frequency factor; for the present purpose, it is adequate to consider it as a constant $\nu \approx 6 \times 10^{12}\ s^{-1}$; k is the Boltzmann constant; T is the absolute temperature; and $\Delta G^{\ddagger}(W)$ is the apparent activation energy.

The apparent activation energy is defined by:

$$\Delta G^{\ddagger}(W) = \Delta G^{\ddagger} \pm W(\tau) = \Delta G^{\ddagger} \pm V\tau \qquad [2]$$

where $\Delta G^{\ddagger}$ is the true activation energy, the energy needed to break atomic bonds and to rearrange the atoms by a specific mechanism of the process; $W = V\tau$ is the mechanical work contributed by the effective shear stress, τ, acting on the dislocation; and V is the activation volume. The sign of $W(\tau)$ and $V\tau$ is defined by the direction of the dislocation movement: It is positive for forward activation and negative for reverse activation. Figure 1 illustrates the change in the height of the energy barrier that controls plastic deformation. The effects of the work on the apparent activation energy of the forward and reverse activation is also demonstrated.

Dislocation velocity represents the net rate of thermal activation over the energy barrier:

$$v = l_f \mathbf{k}_f - l_r \mathbf{k}_r \qquad [3]$$

where l is the activation distance; $\mathbf{k}$ is the activation rate, as expressed by Eq 1, and the subscripts f and r signify forward and reverse activation, respectively.

Substituting Eq 1 to 3 in the Orowan equation

$$\dot{\gamma}_p = b\rho v \qquad [4]$$

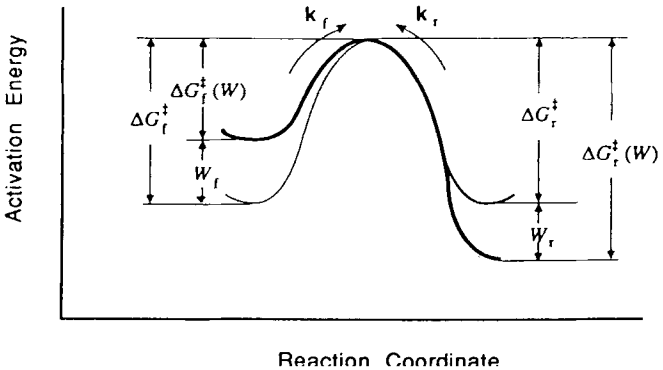

Fig. 1 Schematic of a single energy barrier system.

where $\dot{\gamma}_p$ is the plastic strain rate, p is the dislocation density, and b is the Burger's vector, the strain rate is

$$\dot{\gamma}_p = A_f \exp\left(\frac{V_f \tau}{kT}\right) - A_r \exp\left(-\frac{V_r \tau}{kT}\right) \quad [5]$$

where

$$A_f = \nu b l_f \rho_f exp\left(-\frac{\Delta G_f^{\ddagger}}{kT}\right) and\ A_r = \nu b l_r \rho_r\ exp\left(-\frac{\Delta G_r^{\ddagger}}{kT}\right)$$

Equation 5 has been widely used for the description of plastic deformation.[11-17] It expresses the most general condition that (1) the dislocation density, ρ, (2) the activation energy, $\Delta G^{\ddagger}$, and (3) the activation volume, V, may not be the same in the forward and in the reverse direction. The rate constants, A_f and A_r, usually vary with stress because the dislocation density changes during deformation.[18,19] Dislocation multiplication can affect significantly the yield drop and the time-delay of creep in low activation energy materials such as Ge, LiF, ice, and even in mild steels.[11,20] In high-strength alloys, the activation energy is large, and the stress dependence of the exponential function is so large that the effect of the change in the pre-exponential term can be neglected and A_f and A_r can be considered to be independent of the stress. Under various conditions, Eq 5 can be further simplified. In particular, it is well recognized that in the high-temperature region the energy barrier is symmetrical, and the rate equation reduces to a sinh-type relation.[14-17]

The empirical relation:[21,22]

$$\dot{\gamma}_p = A' \sinh^n \beta\tau \quad [6]$$

was proposed a very long time ago and is still used extensively for the kinetics equation of the constitutive law. In Eq 6, A', β, and n are experimental constants. Equation 6 appears to be a reasonably good description of the behavior exhibited in many tests; however, being an empirical expression, its validity cannot be assumed outside the actually tested range. This limits its application severely. Because the deformation kinetics rate equation (Eq 5) is physically based and rigorously derived, it can be used for extrapolation with confidence and for the physical description of the parameters of the $\sinh^n$ relation (Eq 6). Equating 5 and 6 yields:

$$\dot{\gamma}_p = A' \sinh^n \beta\tau = A' \left[\frac{\exp(\beta\tau) - \exp(-\beta\tau)}{2}\right]^n$$

$$= A_f \exp\left(\frac{V_f \tau}{kT}\right) - A_r \exp\left(\frac{V_r \tau}{kT}\right) \quad [7]$$

At high stresses, the reverse term $A_r \exp\left(-\frac{V_r \tau}{kT}\right)$ and $\exp(-\beta\tau)$ are negligible, i.e.:

$$\frac{A'}{2^n} \exp[n\beta\tau] = A_f \exp\left(\frac{V_f \tau}{kT}\right)$$

From this, it follows that:

$$A' = 2^n A_f \text{ and } n\beta = \frac{V_f}{kT} \quad [8]$$

At low stresses (when $\beta\tau << 1$), the sinh term in Eq 7 reduces to a power-law function:

$$A' \beta^n \tau^n = A_f \exp\left(\frac{V_f \tau}{kT}\right) - A_r \exp\left(-\frac{V_r \tau}{kT}\right) \quad [9]$$

From Eq 9, the exponent is

$$n = \frac{d \ln \dot{\gamma}_P}{d \ln \tau} = \frac{\frac{A_f V_f \tau}{kT} \exp\left(\frac{V_f \tau}{kT}\right) + \frac{A_r V_r \tau}{kT} \exp\left(-\frac{V_r \tau}{kT}\right)}{A_f \exp\left(\frac{V_f \tau}{kT}\right) - A_r \exp\left(-\frac{V_r \tau}{kT}\right)} \quad [10]$$

and from Eq 8 and 10, β is defined as:

$$\beta = \frac{V_f}{nkT} = \frac{1}{\tau}\left[\frac{1 - \frac{A_r}{A_f} \exp\left(-\frac{(V_f + V_r)\tau}{kT}\right)}{1 + \frac{A_r V_r}{A_f V_f} \exp\left(-\frac{(V_f + V_r)\tau}{kT}\right)}\right] \quad [11]$$

Equations 8, 10, and 11 define A', β, and n in terms of rigorously derived physical quantities: The $\dot{\gamma}_p = A' \sinh^n \beta\tau$ relation is now equivalent to the physically based rate equation (Eq 5) and describes the plastic strain rate well.

In applications, the integration of Eq 5 or 6 may be inconvenient when the internal stress, and hence the effective stress, changes with deformation in low-temperature deformation. For the economical evaluation of test results and for the design of components, a constitutive law that incorporates the rigorousness of the deformation kinetics rate equation and the simplicity of the empirical form of the hyperbolic sine model

expressed with physically defined parameters is of advantage. To obtain this form, Eq 5, 6, 9, 10, and 11 are combined to yield:

$$\dot{\gamma}_p = A_f \exp\left(\frac{V_f\tau}{kT}\right) - A'_r \exp\left(-\frac{V_f\tau}{kT}\right) \quad [12]$$

Equation 12 is in formal agreement with the rigorously derived equation (Eq 5) at the condition that the work is the same in forward and reverse activations. In Eq 12, A'_r is an activation parameter that can be determined by expressing the threshold condition $\dot{\gamma}_p = 0$ from Eq 5 and 12:

$$\tau_{th} = \frac{kT}{V_f + V_r} \ln \frac{A_r}{A_f} = \frac{kT}{2V_f} \ln \frac{A'_r}{A_f} \quad [13]$$

From this, it follows that:

$$A'_r = A_f \left(\frac{A_r}{A_f}\right)^{\frac{2V_f}{V_f+V_r}}$$

In the high strain rate range, the reverse rate terms are negligible, and Eq 5 and 12 are identical. In the low range, the difference between the two is

$$\frac{\Delta\dot{\gamma}_p}{\dot{\gamma}_p} = \frac{A'_r \exp\left(-\frac{V_f\tau}{kT}\right) - A_r \exp\left(-\frac{V_r\tau}{kT}\right)}{A_f \exp\left(\frac{V_f\tau}{kT}\right) - A_r \exp\left(-\frac{V_r\tau}{kT}\right)}$$

$$= \frac{A_f \exp\left(-\frac{V_f(\tau - 2\tau_{th})}{kT}\right) - A_r \exp\left(-\frac{V_r\tau}{kT}\right)}{A_f \exp\left(\frac{V_f\tau}{kT}\right) - A_r \exp\left(-\frac{V_r\tau}{kT}\right)}$$

$$= \frac{A_f \exp\left(\frac{V_f\tau_{th}}{kT}\right) - A_r \exp\left(-\frac{V_r\tau_{th}}{kT}\right) \exp\left(\frac{(V_f - V_r)(\tau - \tau_{th})}{kT}\right)}{A_f \exp\left(\frac{V_f\tau}{kT}\right) - A_r \exp\left(-\frac{V_r\tau}{kT}\right)}$$

$$\exp\left(-\frac{v_f(\tau - \tau_{th})}{kT}\right)$$

where $\Delta\dot{\gamma}_p$ represents the difference between Eq 5 and 12.

Typically for $|V_r - V_f| < 10\ b^3$ (the lower limit for Peierls-Nabarro mechanism[11]), $\tau - \tau_{th} < 30$ MPa (about one third of Orowan stress, which characterizes the threshold condition[10]) and T = 300 K:

$$\exp\left(-\frac{(V_r - V_f)(\tau - \tau_{th})}{kT}\right) \approx 1 - \frac{(V_r - V_f)(\tau - \tau_{th})}{kT}$$

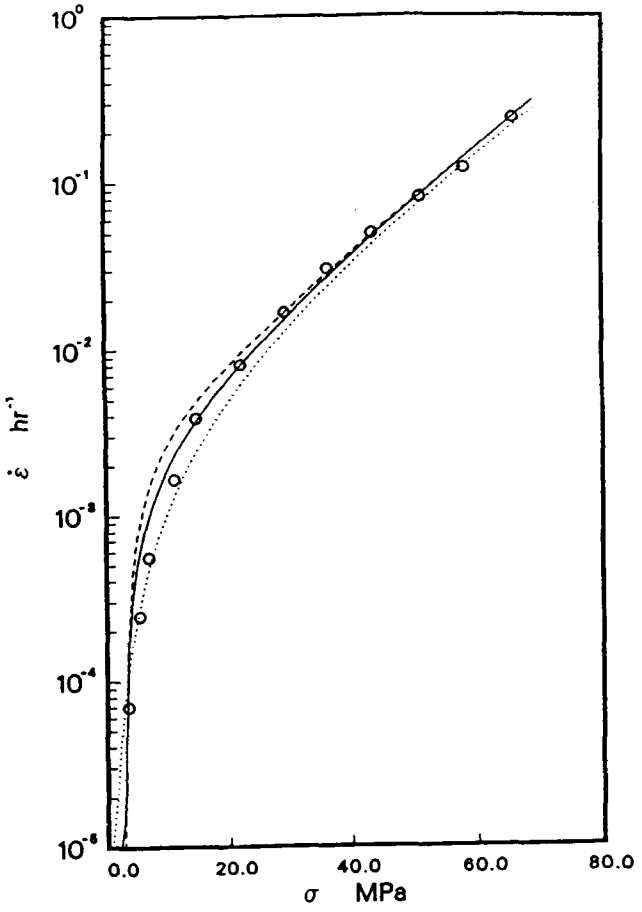

Fig. 2 Typical strain rate versus stress relation. The solid line represents Eq 5, with $A_f = 2 \times 10^{-3}$, $V_f/kT = 0.073$, $A_r = 2.5 \times 10^{-3}$, and $V_r/kT = 0.01$. The dotted line represents Eq 6, with $A' = 9.17 \times 10^{-3}$, $\beta = 0.034$, and $n = 2.06$. The dashed line represents Eq 12, with $A_f = 2 \times 10^{-3}$, $A_r = 3 \times 10^{-3}$, and $V/kT = 0.073$. The symbols represent the observed behavior.[21]

The error reduces to (the condition $\dot{\gamma}_p = 0$ at $\tau = \tau_{th}$ has been used):

$$\frac{|\Delta\dot{\gamma}_p|}{\dot{\gamma}_p} = \frac{\frac{|V_r - V_f|(\tau - \tau_{th})}{kT} A_r \exp\left(-\frac{V_r\tau_{th}}{kT}\right) \exp\left(-\frac{V_f(\tau - \tau_{th})}{kT}\right)}{A_f \exp\left(\frac{V_f\tau}{kT}\right) - A_r \exp\left(-\frac{V_r\tau}{kT}\right)}$$

$$= \frac{\frac{|V_r - V_f|(\tau - \tau_{th})}{kT} \exp\left(-\frac{V_f(\tau - \tau_{th})}{kT}\right)}{\exp\left(\frac{V_f(\tau - \tau_{th})}{kT}\right) - \exp\left(-\frac{V_r(\tau - \tau_{th})}{kT}\right)}$$

which approaches to $|V_r - V_f|/(V_r + V_f) < 1$ as $\tau \to \tau_{th}$ and diminishes rapidly with increasing stress. Because in the threshold region strain rate measurements have a scatter factor of about 4, Eq 12 is a good approximation of the general equation (Eq 5) within the specified error range. Figure 2 illustrates the strain rate defined by Eq 5 and 12 together with the empirical equation (Eq 6) measured in an Al-Mg alloy.[21] All curves fall within the ±2 band that envelopes the experimental data.

Letting $V_f = V_r = V$, both Eq 5 and Eq 12 become:

$$\dot{\gamma}_p = \sqrt{A_f A_r}\left[\exp\left(\frac{V(\tau - \tau_{th})}{kT}\right) - \exp\left(-\frac{V(\tau - \tau_{th})}{kT}\right)\right]$$

which can be expressed as a hyperbolic sine function:

$$\dot{\gamma}_p = 2A \sinh\frac{V(\tau - \tau_{th})}{kT} \qquad [14]$$

where

$$A = \sqrt{A_f A_r} = b\nu\sqrt{l_f l_r \rho_f \rho_r}\exp\left(-\frac{\Delta G_f^{\ddagger} + \Delta G_r^{\ddagger}}{2kT}\right)$$

During deformation, polycrystalline materials often undergo work hardening. For small strains,[20] the effective stress can be expressed as:

$$\tau_{eff} = \tau - \tau_i = \tau - H\gamma - \tau_{i0} \qquad [15]$$

where τ_i is the internal stress; τ_{i0} is the initial internal stress; and H is the work-hardening coefficient.

Substituting the effective stress from Eq 15 into Eq 14, the rate equation is

$$\dot{\gamma}_p = 2A \sinh\frac{V(\tau - H\gamma_p - \tau_0)}{kT} \qquad [16]$$

where

$$\tau_0 = \tau_{i0} + \tau_{th} = \tau_{i0} + \frac{kT}{2V}\ln\frac{A_r}{A_f} \qquad [17]$$

3. Application—Operational Equations

Define a normalized energy function Φ as:

$$\Phi = \frac{V}{kT}(\tau - H\gamma_p - \tau_0) \qquad [18]$$

By definition, Φ is the effective activation work normalized with thermal energy content kT. Because the activation parameters (A_f, A_r, V, and τ_{i0}) and the work-hardening coefficient, H, are microstructural quantities, the function Φ depends on the current stress, the accumulated plastic strain, and the temperature. The evolution of function Φ controls the deformation response. For an isothermal process, the small-strain deformation is governed by:

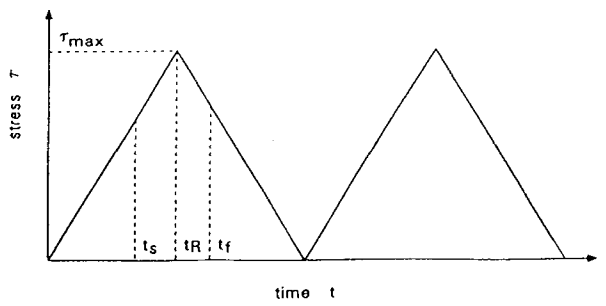

Fig. 3 Triangular wave loading profile; t_R is the stress rising time.

$$\dot{\gamma} = \frac{\dot{\tau}}{\mu} + \dot{\gamma}_p \qquad [19]$$

$$\dot{\gamma}_p = 2A \sinh\Phi \qquad [20]$$

$$\dot{\Phi} = \frac{V}{kT}(\dot{\tau} - H\dot{\gamma}_p) \qquad [21]$$

$\gamma = \gamma_e + \gamma_p$, where $\gamma_e = \tau/\mu$ (μ is the shear modulus) is the elastic strain, and γ_p is the plastic strain. The shear strain, γ, can be converted to the normal strain, ε, with the relation[10] $\varepsilon = \gamma/\sqrt{3}$, and the shear stress τ can be converted to the normal stress σ with[10] $\sigma = \sqrt{3}\tau$.

By imposing the loading constraint, the evolutionary equation (Eq 20) and Eq 21 can be solved to yield the operational equation that describes stress-strain, stress-time, and strain-time response.

3.1. *Constant Strain-Rate Loading*

At constant strain rate, Eq 19 yields:

$$\dot{\tau} = \mu(\dot{\gamma} - \dot{\gamma}_p)$$

Substituting this and the rate equation (Eq 20) into Eq 21:

$$\dot{\Phi} = \frac{V\mu\dot{\gamma}}{kT}\left[1 - \left(1 + \frac{H}{\mu}\right)\frac{2A}{\dot{\gamma}}\sinh\Phi\right] \qquad [22]$$

Equation 22 can be integrated to:

$$\frac{u - a}{\chi u + b} = \frac{1 - a}{\chi + b}\exp\left(-\frac{V\mu\dot{\gamma}t\sqrt{1 + \chi^2}}{kT}\right) \qquad [23]$$

where

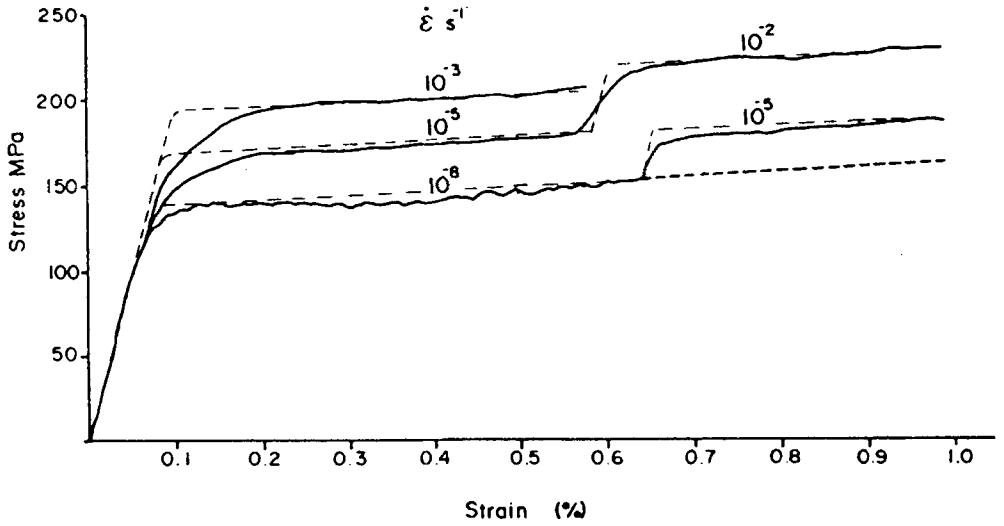

Fig. 4 Stress-strain response in type 304 stainless steel.[23] The solid lines represent the test behavior. The dashed lines represent Eq 24, with $\tau_0 = 55.32$ MPa, $H = 718.33$ MPa, $V/kT = 0.43$ MPa^{-1}, and $\chi = 2 \times 10^{-13}/\dot{\varepsilon}$.

$$\chi = \frac{2A}{\dot{\gamma}}\left(1+\frac{H}{\mu}\right), a = \frac{\sqrt{1+\chi^2}-1}{\chi}, b = \frac{\sqrt{1+\chi^2}+1}{2}$$

and

$$u = \exp -\Phi$$

After a short elastic-plastic transient, Φ reaches a steady value of

$$\Phi_s = \frac{V}{kT}(\tau - H\gamma_p - \tau_0) = -\ln\frac{\sqrt{1+\chi^2}-1}{\chi} \quad [24]$$

Equation 24 describes the stress-strain response in the range of plastic deformation. By back-extrapolation, the yield stress can be obtained at $\gamma_p = 0$ as:

$$\tau_y = \tau_0 - \frac{kT}{V}\ln\frac{\sqrt{1+\chi^2}-1}{\chi} \quad [25]$$

For more complicated yielding behavior, e.g., for yield drop phenomena, a dislocation multiplication model has to be incorporated into the kinetics description.[11,19,20] In that case, the differential equation (Eq 22) has to be solved numerically.

3.2. *Stress Relaxation*

In stress relaxation, the total strain is held at a constant value so that:

$$\dot{\gamma} = \frac{\dot{\tau}}{\mu} + \dot{\gamma}_P = 0$$

Equation 21 then reduces to:

$$\dot{\Phi} = -\frac{V(\mu+H)}{kT}\dot{\gamma}_p = -\frac{2V(\mu+H)A}{kT}\sinh\Phi \quad [26]$$

which can be integrated to the form:

$$\tanh\left(\frac{\Phi}{2}\right) = \tanh\left(\frac{\Phi_o}{2}\right)\exp\left(-\frac{2V(\mu+H)At}{kT}\right) \quad [27]$$

From this, the stress variation in stress relaxation can be expressed as:

$$\tau = \tau_i + \frac{2kT}{V}\tanh^{-1}\left[\tanh\left(\frac{\Phi_o}{2}\right)\exp\left(-\frac{2V(\mu+H)At}{kT}\right)\right] \quad [28]$$

3.3. *Constant Stress-Rate Loading and Ratchetting*

Consider a triangular-wave loading profile, as shown in Fig. 3, where t_s represents the starting time of plastic flow and t_f the final time of plastic flow, both satisfying the condition $\Phi = 0$.

In the loading period ($t_s \le t \le t_R$):

$$\dot{\Phi} = \frac{V}{kT}(\dot{\tau} - H\dot{\gamma}_p) = \frac{V\dot{\tau}}{kT}\left(1 - \frac{2AH}{\dot{\tau}}\sinh\Phi\right) \quad [29]$$

which can be integrated to

$$\frac{u-p}{\lambda u+q} = \frac{1-p}{\lambda+q}\exp\left(-\frac{V\dot{\tau}\sqrt{1+\lambda^2}\,(t-t_s)}{kT}\right) \quad [30]$$

where

$$\lambda = \frac{2AH}{\dot{\tau}}, p = \frac{\sqrt{1+\lambda^2}-1}{\lambda}, q = \frac{\sqrt{1+\lambda^2}+1}{2}$$

$u = \exp -\Phi$

In the unloading period ($t_R \le t \le t_f$):

$$\dot{\Phi} = -\frac{V}{kT}(\dot{\tau} + H\dot{\gamma}_p) = -\frac{V\dot{\tau}}{kT}\left(1 + \frac{2AH}{\dot{\tau}} \sinh \Phi\right) \qquad [31]$$

which can be integrated to

$$\frac{u+p}{q-\lambda u} = \frac{u_R + p}{q - \lambda u_R} \exp\left(-\frac{V\dot{\tau}\sqrt{1+\lambda^2}\,(t_R - t)}{kT}\right) \qquad [32]$$

where $u_R = \exp -\Phi\,(t_R)$ is determined by Eq 30 at $t = t_R$.

In stress-controlled cycling, materials often exhibit ratchetting behavior in which the plastic strain accumulates progressively. The small amount of plastic strain that is not reversed in the cycles may lead to unacceptably large accumulated strains. For this condition, Eq 30 and 32 provide a set of iterative equations that express the accumulated plastic strain. Although Eq 30 and 32 are derived for the zero-to-tension loading case, they are also valid for loading with a positive stress ratio ($R = \tau_{min}/\tau_{max}$), provided the minimum stress does not exceed τ_0.

At low temperatures, λ is small and then Eq 30 and 32 can be combined in a differential form (see Appendix A for details):

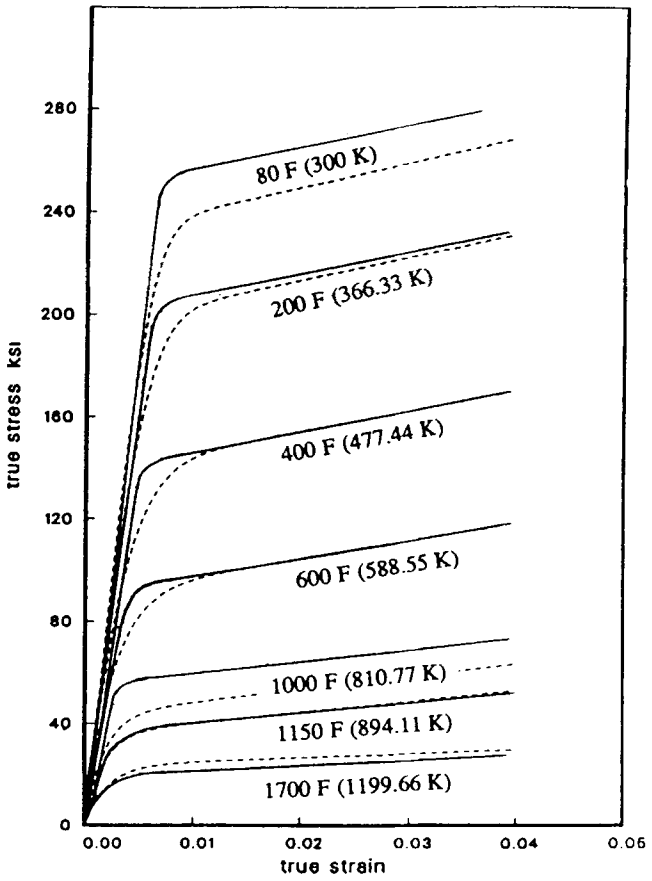

Fig. 5 Stress-strain curves for 8660 steel.[24] The solid lines represent the observed behavior. The dashed lines represent Eq 23, with $\chi = 66.97 \exp(-2589/T)$, $V/k = 6.5$. The elastic modulus E and work-hardening coefficient H vary with the temperature as $E = 40000\,(1 - 0.0008\,[T - 300])$ and $H = 963\,(1 - 0.00093\,[T - 300])$. Temperature is in degrees Kelvin.

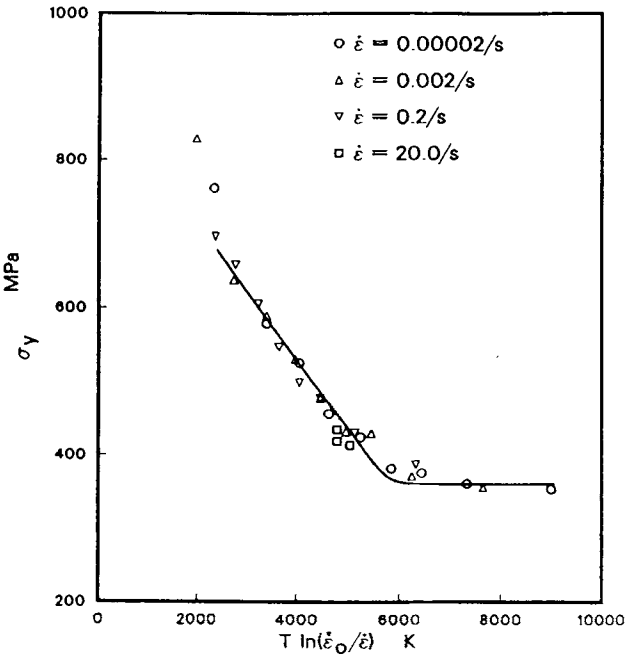

Fig. 6 Yield stress as a function of strain rate and temperature. The symbols represent the behavior of a microalloyed steel[16] and the curve represents Eq 25:
$\sigma_y = 359.54 - 0.0942T \ln\{[\sqrt{(1+\chi^2)} - 1]/\chi\}$
where $\chi = (5.4 \times 10^8/\dot{\epsilon}) \exp(-5800/T)$.

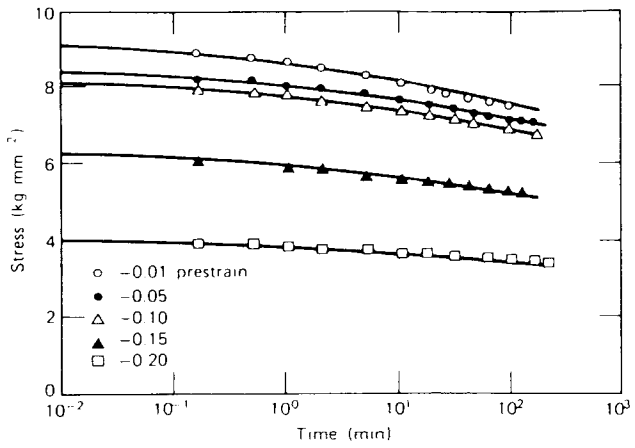

Fig. 7 Stress relaxation in 1100 aluminum.[15]

$$\frac{d\gamma_p}{dN} = \frac{kT}{VH}\left[\Phi + \ln\left(\frac{2AH}{\dot{\tau}} + \exp(-\Phi)\right)\right]$$

$$\Phi = \frac{V}{kT}(\tau_{max} - H\gamma_p - \tau_0) \quad [33]$$

3.4. *Creep*

In creep, $\dot{\tau} = 0$ and Eq 21 reduce to:

$$\dot{\Phi} = -\frac{VH}{kT}\dot{\gamma}_p = -\frac{2VHA}{kT}\sinh\Phi \quad [34]$$

which can be integrated to:

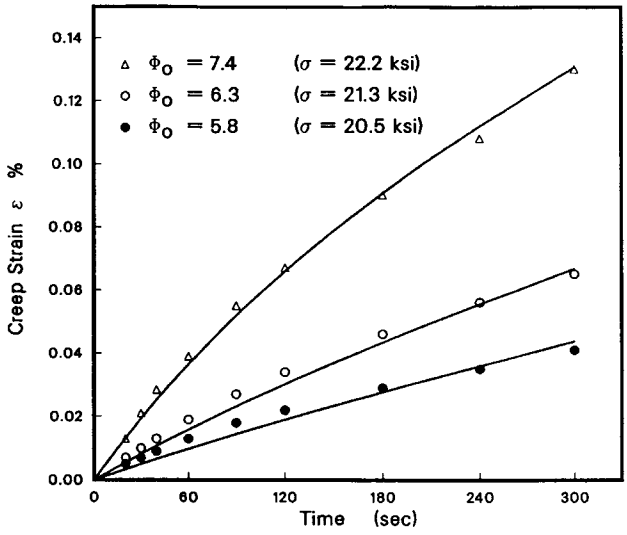

Fig. 8 Comparison of Eq 35 with the creep behavior of type 304 stainless steel tested at room temperature.[23] The creep strain is given by $\varepsilon = (\Phi_0 - \Phi)/\sqrt{3}VH$, where Φ is obtained from Eq 35 with $V/kT = 0.52\ \text{MPa}^{-1}$, $H = 718.33$ MPa, and $2VHA/kT = 6.6 \times 10^{-6}$.

$$\tanh\left(\frac{\Phi}{2}\right) = \tanh\left(\frac{\Phi_0}{2}\right)\exp\left(-\frac{2VHAt}{kT}\right) \quad [35]$$

4. Comparison and Discussion

Plastic deformation is always rate and temperature dependent—it is thermally activated.[23-25] Analyses of experimental results obtained in tensile tests demonstrate that Eq 23 and 24 represent the behavior over a wide strain rate and temperature range. Figure 4 represents the behavior of type 304 stainless steel at three strain rates,[23] and Fig. 5 shows the effect of temperature on the stress-strain relation in 860 steel.[26] The variation of yield stress with strain rate and temperature is shown in Fig. 6. Good agreement with the constitutive law is noted.

Table 1 Material constants and activation parameters for type 304 stainless steel

Material constants	
μ	5766.4 MPa
H	718.33 MPa
$V/\sqrt{3}$	1.213×10^{-21} cm^3
$A/\sqrt{3}$	5.08×10^{-9} s^{-1}

Table 2 Comparison of calculations and measurements

Mechanical quantities	Test	Calculation	Test	Calculation
t_R, s	2	2	210	210
σ_A, MPa	217	219	209	219
ε_{RAT}, %	0.561	0.575	1.139	1.286
ε_{CR}, %	0.365	0.386	0.018	0.016
ε_F, %	1.810	1.834	2.039	2.176
σ_G, MPa	257	258.5	256	258
ε_{SC}, %	0.702	0.6	0.847	0.733

Note: σ_A is the stress at point A; σ_G is the stress at point G; ε_{RAT} is the ratchet strain accumulated from point B to C; ε_{CR} is the creep strain in DE; ε_F is the plastic strain at point G; and ε_{SC} is the plastic strain produced by load sequence HI.

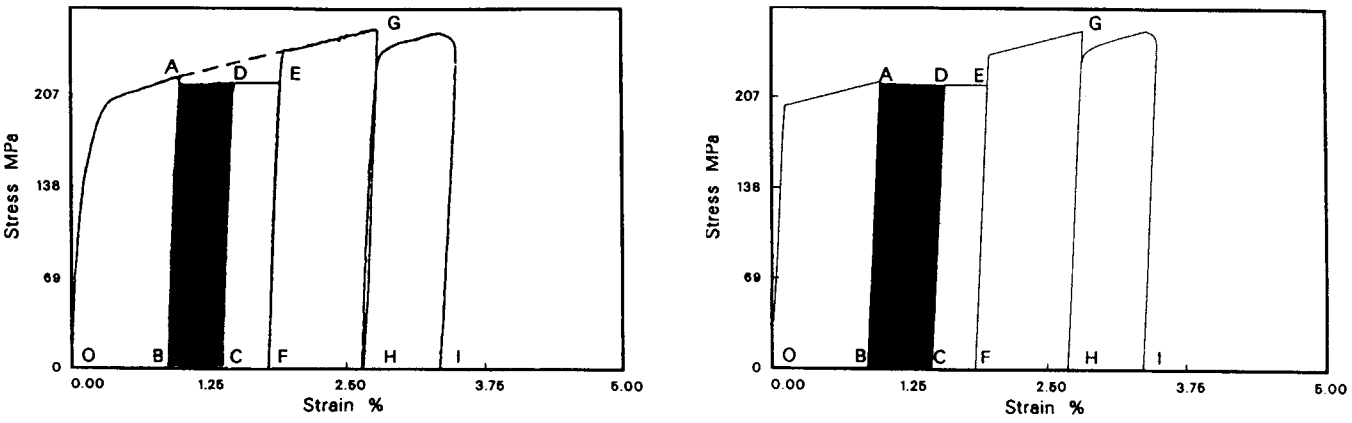

Fig. 9 Stress-strain curve for type 304 stainless steel. (a) Experimental.[27] (b) Predicted.

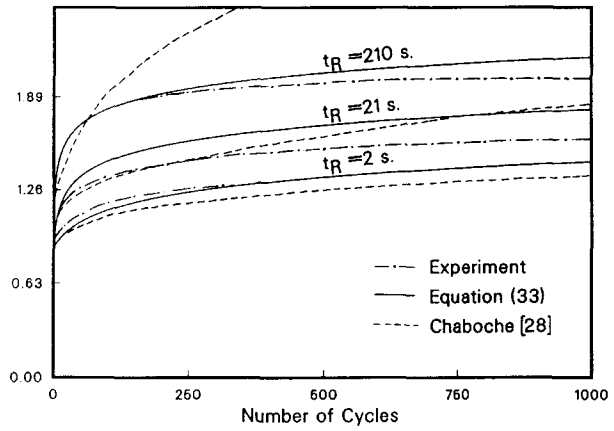

Fig. 10 Rate dependence of ratchet strain under stress cycling. The symbols represent the test results.[27] The solid curves are descriptions of Eq 33, and the dashed curves are descriptions of Chaboche's model.[28]

The behavior in stress relaxation in expressed by Eq 27. Stress relaxation tests provide a method for the determination of the internal stress. As shown by Eq 27, τ_i is the stress level at the end of stress relaxation. The stress relaxation of a 1100 aluminum alloy was analyzed by Wilson and Garofalo[14,15] using a kinetic equation similar to Eq 28 for a symmetrical barrier. Their results are shown in Fig. 7.

Creep was also analyzed. Equation 35 shows that the initial value of Φ controls the subsequent creep: It depends on the stress, temperature, and the initial strain. Figure 8 shows the creep behaviors of type 304 stainless steel at three stress levels. Very good agreement is found between the theoretical description (Eq 29) and the observed behavior.

The validity of the deformation kinetics model can be further verified by a simulated test on type 304 stainless steel in comparison with the actual experiments of Ruggles and Krempl.[27] The imposed loading sequence (History I) are OA—strain-controlled loading to $\varepsilon = 1\%$ with strain rate $\dot{\varepsilon} = 8.33 \times 10^{-4}\ s^{-1}$; AD—stress-controlled cycling (1000 cycles) with a rise time of 2 s; DE—creep for 700 s; FG—strain-controlled loading to $\varepsilon F + 1\%$ strain; and HI—one cycle of stress-controlled cycling (2100 s). These processes are described by Eq 17, 24, 26, 27, and 29, with material constants and activation parameters as listed in Table 1. The measured behavior is shown in Fig. 9(a), and the calculated stress-strain response is shown in Fig. 9(b). The measured and calculated behavior is also given in Table 2. Excellent agreement was found between the theoretical description and the experiment.

In stress-controlled cycling, materials often exhibit significantly rate-dependent ratchetting behavior.[27] The classical treatment applies either time-independent plasticity or plasticity.[28] Equation 33 provides a theoretical description developed from deformation kinetics theory; it expresses the strain increment per cycle ($d\gamma/dN$) explicitly in terms of stress, temperature, and loading rate. Figure 10 shows the comparisons of Eq 33 with the observed behavior and a power-law model.[28] It is obvious that deformation kinetics theory provides a good description of ratchetting.

5. Conclusions

It has been shown that low-temperature plastic deformation can be represented by kinetics combination of forward and reverse activations (Eq 5). From Eq 5, the empirical $\sinh^n$ equation (Eq 6) is derived in physically rigorous terms. The hyperbolic sine expression (Eq 14) is equivalent to the general rate equation (Eq 5) under the condition that the activation work is equal in forward and reverse directions.

An energy function

$$\Phi = \frac{V}{kT}(\tau - H\gamma_p - \tau_0)$$

was introduced. Plastic deformation processes are shown to be governed by the evolution of this energy expression and the strain-rate equation (Eq 20) coupled with the evolutionary equation (Eq 21). Because the apparent activation energy $\Delta G^{\ddagger}(W)$ is related to the function Φ through the relationship

$$\Delta G^{\ddagger}(W) = \Delta G^{\ddagger} - W_{eff} = \Delta G^{\ddagger} - kT\Phi$$

this energy approach is uniquely defined by the principles of statistical thermodynamics. The differential equations (Eq 20 and 21) represent the plastic flow and the energy condition; the operational equations describe the deformation response to the imposed loading constraints.

Acknowledgment

The financial support provided by the Natural Sciences and Engineering Council of Canada is gratefully acknowledged.

References

1. M. Polanyi and E. Schmid, *Z. Physik.*, Vol 16, 1923, p 336
2. E. Orowan, *Proc. Phys. Soc.*, Vol 52, 1940, p 8
3. J.E. Dorn, in *Dislocation Dynamics*, McGraw-Hill, 1967, p 27
4. V. Celli, M. Kabler, T. Ninomiya, and R. Thomson, *Phys. Rev.*, Vol 131, 1963, p 58
5. J.E. Dorn and S. Rajnak, *Trans. Metall. Soc. AIME*, Vol 230, 1964, p 1052
6. P. Guyot and J.E. Dorn, *Can. J. Phys.*, Vol 45, 1967, p 983
7. J.P. Hirth, in *Inelastic Behavior of Solids*, McGraw-Hill, 1970, p 281
8. A.S. Krausz and B. Faucher, *Scrip. Metall.*, Vol 13, 1979, p 91
9. U.F. Kocks, A.S. Argon, and M.F. Ashby, *Prog. Mater. Sci.*, Vol 19, 1975
10. H.J. Frost and M.F. Ashby, *Deformation Mechanism Maps*, Pergamon Press, 1982
11. A.S. Krausz and H. Eyring, *Deformation Kinetics*, Wiley-Interscience, 1975
12. D. Caldwell and H. Eyring, *Perspectives in Quantum Theory*, Dover Publications, 1972, p 117
13. A.S. Krausz and B. Faucher, in *Rev. Deform. Behav. Mater.*, Vol 4, 1982, p 105
14. J.F. Wilson and F. Garofalo, *Mater. Res. Stand. ASTM*, Vol 6, 1966, p 85
15. J.F. Wilson and N.K. Wilson, *Trans. Soc. Rheol.*, Vol 10, 1966, p 399

16. B. Faucher and W.R. Tyson, in *Constitutive Laws of Plastic Deformation and Fracture*, 19th Canadian Fracture Conference, Ottawa, 1989, p 27-1
17. B.F. Dyson, in, *Modelling of Material Behavior and Design*, TMS, 1990, p 59
18. A.S. Argon, *Scrip. Metall.*, Vol 4, 1970, p 1001
19. W.G. Johnston and J.J. Gilman, *J. Appl. Phys.*, Vol 30, 1959, p 129
20. W.G. Johnston, *J. Appl. Phys.*, Vol 33, 1961, p 2716
21. F. Garofalo, *Trans. AIME*, Vol 227, 1963, p 351
22. A.G. Guy, *Introduction to Materials Science*, McGraw-Hill, 1972
23. E. Krempl, *J. Mech. Phys. Solids*, Vol 27, 1979, p 363
24. V.G. Ramaswamy, D.C. Stouffer, and J.H. Laflen, *J. Eng. Mater. Tech.*, Vol 112, 1990, p 280
25. L.A. Lalli and A.J. DeArdo, *Metall. Trans. A*, Vol 21, 1990, p 3101
26. J. Larry, Ed., *Residual Stress for Designers and Metallurgists*, American Society for Metals, 1981, p 56
27. M.B. Ruggles and E. Krempl, *J. Eng. Mater. Tech.*, Vol 111, 1989, p 378
28. J.L. Chaboche and D. Nouailhas, *J. Eng. Mater. Tech.*, Vol 111, 1989, p 406

Appendix A

Let $\gamma_p(i)$ denote the accumulated plastic strain after i cycle. In the n-th cycle, plastic flow starts at t_s when

$$\Phi(t_s) = \frac{V}{kT}[\tau_{max} - \dot{\tau}(t_R - t_s) - H\gamma_p(n-1) - \tau_0] = 0 \quad [36]$$

and ceases at t_f when

$$\Phi(t_f) = \frac{V}{kT}[\tau_{max} - \dot{\tau}(t_f - t_R) - H\gamma_p(n) - \tau_0] = 0 \quad [37]$$

From Eq 32:

$$t_f - t_R = \frac{kT}{V\dot{\tau}\sqrt{1+\lambda^2}} \ln \frac{(1+p)(q-\lambda u_R)}{(q-\lambda)(u_R+p)} \quad [38]$$

Substituting Eq 38 into Eq 37 and by rearrangement:

$$\gamma_p(n) - \gamma_p(n-1) = \frac{1}{H}\left[\tau_{max} - H\gamma_p(n-1) - \tau_0\right] - \frac{kT}{HV\sqrt{1+\lambda^2}} \ln \frac{(1+p)(q-\lambda u_R)}{(q-\lambda)(u_R+p)} \quad [39]$$

where u_R can be obtained from Eq 30 as:

$$\frac{u_R - p}{\lambda u_R + q} = \frac{1-p}{\lambda+q} \exp\left(-\frac{V\dot{\tau}\sqrt{1+\lambda^2}\,(t_R - t_s)}{kT}\right)$$

$$= \frac{1-p}{\lambda+q} \exp\left(-\frac{V\sqrt{1+\lambda^2}\,[\tau_{max} - H\gamma_p(n-1) - \tau_0]}{kT}\right)$$

At low temperatures where $\lambda << 1$, then $p \cong \lambda/2$, $q \cong 1$, and

$$u_R \cong p + \exp\left(-\frac{V[\tau_{max} - H\gamma_p(n-1) - \tau_0]}{kT}\right)$$

Eq 39 reduces to:

$$\Delta\gamma_p = \frac{kT}{VH}\left[\Phi(n-1) + \ln\left(\frac{2AH}{\dot{\tau}} + \exp[-\Phi(n-1)]\right)\right] \quad [40]$$

where

$$\Delta\gamma_p = \gamma_p(n) - \gamma_p(n-1)$$

$$\Phi(n-1) = \frac{V}{kT}[\tau_{max} - H\gamma_p(n-1) - \tau_0]$$

Writing Eq 40 in a continuous form results in:

$$\frac{d\gamma_p}{dN} = \frac{kT}{VH}\left[\Phi + \ln\left(\frac{2AH}{\dot{\tau}} + \exp(-\Phi)\right)\right]$$